(15) Leermakers, F. A. M.; Scheutjens, J. M. H. M.; Gaylord, R. J. *Polymer* **1984**, *25*, 1577.
(16) Kurata, M.; Isida, S.-I. *J. Chem. Phys.* **1954**, *23*, 1126.
(17) van Voorhis, J. J.; Craig, R. G.; Bartell, F. E. *J. Phys. Chem.* **1957**, 1513.
(18) Ash, S. G.; Everett, D. H.; Radke, C. *J. Chem. Soc., Faraday Trans. 2* **1973**, *69*, 1256.
(19) Helfand, E.; Sapse, A. M. *J. Polym. Sci., Polym. Symp.* **1976**, *54*, 289.
(20) Ploehn, H. J.; Russel, W. B.; Hall, C. K. *Macromolecules* **1988**, *21*, 1075.
(21) Rabin, Y. *J. Polym. Sci., Polym. Lett. Ed.* **1984**, *22*, 335.
(22) Bongiorno, V.; Scriven, L. E.; Davis, H. T. *J. Colloid Interface Sci.* **1976**, *57*, 462.
(23) Jasper, J. J. *J. Phys. Chem. Ref. Data* **1972**, *1*, 841.
(24) Legrand, D. G.; Gaines, G. L. *J. Colloid Interface Sci.* **1969**, *31*, 162.
(25) Roe, R.-J. *J. Phys. Chem.* **1968**, *72*, 2013.
(26) Van Krevelen, D. W. *Properties of Polymers*; Elsevier: Amsterdam, 1976.
(27) Hillstrom, K. *Nonlinear Optimization Routines in AMDLIB*; Technical Memorandum No. 297, Argonne National Laboratory, Applied Mathematics Division, 1976; Subroutine SBROWN in AMDLIB, 1976, Argonne, IL.
(28) Flory, P. J. *Statistical Mechanics of Chain Molecules*; Interscience: New York, 1969.
(29) Weber, T. A.; Helfand, E. *J. Chem. Phys.* **1980**, *72*, 4014.
(30) Madden, W. G.; Pesci, A. I.; Freed, K. F., submitted to *J. Chem. Phys.*
(31) Professor Matthew Tirrell, personal communication.
(32) Dickman, R. D.; Hall, C. K. *J. Chem. Phys.* **1986**, *85*, 4108.
(33) Dee, G. T.; Walsh, D. T. *Macromolecules* **1988**, *21*, 811, 815.
(34) Mansfield, K. F.; Theodorou, D. N. *Polym. Prepr. (Am. Chem. Soc., Div. Polym. Chem.)* **1988**, *29*(2), 409.

# Variable-Density Model of Polymer Melt/Solid Interfaces: Structure, Adhesion Tension, and Surface Forces

**Doros N. Theodorou**

*Department of Chemical Engineering, University of California, Berkeley, and Center for Advanced Materials, Lawrence Berkeley Laboratory, Berkeley, California 94720.*
*Received December 27, 1988; Revised Manuscript Received April 24, 1989*

ABSTRACT: A recently developed variable-density lattice model is used to predict the macroscopic wetting and spreading behavior of a polymeric liquid on smooth solid surfaces. The force field exerted by the solid affects structural features in the interfacial region. Near strongly adsorbing, "high-energy" solids, polymer density is enhanced relative to the bulk. Conformations are pronouncedly flattened; they relax monotonically to their unperturbed characteristics over a thickness commensurate with the root mean squared end-to-end distance. Near weakly adsorbing solids, polymer density is depleted due to entropic restrictions, and structure is reminiscent of a free polymer surface. A thermodynamic formulation is developed for predicting the forces exerted between molecularly smooth solid surfaces immersed in polymeric liquids, at separations commensurate with chain dimensions. The system considered is a monodisperse 50-unit poly(dimethylsiloxane) between smooth flat plates or crossed cylinder surfaces of various adsorbing strengths. In the case of high-energy solid surfaces, which are most representative of the mica actually used in surface force experiments, the model predicts repulsive forces of negligible magnitude (on the order of 1 $\mu$N/m) due to the polymer. The model indicates that the long-range repulsive forces observed recently with higher molecular weight polymer melts are nonequilibrium (hydrodynamic) in nature.

## 1. Introduction

Understanding the structure and thermodynamics of macromolecular liquids in the vicinity of solid surfaces is important in technical areas such as adhesion, lubrication, and polymer melt processing. A quantitative theory, relating the chemical constitution of polymer chains and the composition and topography of solid surfaces to macroscopic interfacial properties, would be valuable as a tool for the efficient design of multiphase materials containing polymers. With the trend toward miniaturization that prevails in present-day high-technology areas, the need to understand interfacial properties at the molecular level becomes imperative. Polymer phases are becoming so thin that their behavior can no longer be satisfactorily described by continuum approaches.

In a companion paper,[1] we have outlined a variable-density, mean field lattice theory of polymer melt surfaces and polymer melt/solid interfaces. We have also presented some applications to free polymer melt surfaces. Our purpose in this paper is to explore systems involving polymer melt/solid interfaces. Such interfaces have scarcely been examined theoretically, although, from the point of view of applications, they are more interesting than free polymer surfaces. The material presented herein falls under three general headings. Section 2 addresses the problem of predicting molecular organization and adhesion tension at interfaces between a bulk polymer phase and a smooth solid. Section 3 is concerned with very thin polymer films, formed between smooth solid surfaces immersed in a macromolecular liquid. Forces between such surfaces at separations commensurate with chain dimensions have recently been measured; we apply our lattice approach to predict these forces at thermodynamic equilibrium. Results obtained in the bulk melt/solid interface case and in the confined thin-film case are discussed in section 4.

## 2. Modeling the Polymer Melt/Solid Interface

**Adhesion Tension.** As described in the preceding paper in this issue, our interfacial model combines ideas from the equation of state work of Sanchez and Lacombe[2] and from the Scheutjens and Fleer model of polymer adsorption from solution on solid surfaces.[3] The chemical constitution of the polymer is summarized in three molecular parameters: the chain length $r$, the characteristic temperature of cohesive segment–segment interactions $T^*$, and the characteristic pressure $P^*$, from which segmental volume can be extracted. Conformational energy (chain stiffness) effects will not be considered in any of the calculations reported in this paper. Attractive segment/solid interactions, characterized in our lattice model by the parameter $T_s^*$, play a decisive role in shaping the interfacial picture. All computations in this section were performed with a film thickness $h$ large enough that the

0024-9297/89/2222-4589$01.50/0 

middle region is indistinguishable from bulk polymer. Results are thus representative of a single polymer melt/smooth solid interface.

To quantitatively assess the role of adsorptive segment/solid interactions, we adopt the following strategy: We take the exact model "sample" of 50-unit PDMS that was studied in ref 1 (parameter values $r = 256$, $T^* = 476$ K, $P^* = 302$ MPa, $T_L = T_V = 0$), and bring it in contact with a series of smooth solid surfaces of different adsorbing strengths. The unperturbed root mean squared end-to-end distance (equivalently, the unperturbed root mean squared radius of gyration) constitutes an important molecular length scale. Based on a characteristic ratio of 6.2 for poly(dimethylsiloxane) chains[4] and a Si–O bond length of 1.64 Å, the unperturbed root mean squared end-to-end distance of a 50-unit PDMS is estimated as $\langle r^2\rangle_0^{1/2} = 41$ Å. In the Sanchez–Lacombe representation used here, model chains are freely jointed sequences of $r - 1 = 255$ bonds, each of length $l^* = 2.79$ Å. The end-to-end distance of the model chains is thus $(r-1)^{1/2}l^* = 45$ Å, not far from the experimental value. The unperturbed root mean squared radius of gyration $\langle s^2\rangle_0^{1/2}$ is 17 Å for actual 50-unit PDMS chains and 18 Å for our model chains.

A useful thermodynamic property, obtainable from our model,[1] is adhesion tension. Introducing the subscripts f and fs to distinguish between free polymer surface tension and solid/polymer interfacial tension, respectively, and denoting the surface tension of the clean (pure) solid as $\gamma_s$, we define adhesion tension[1] as the difference $\gamma_s - \gamma_{fs}$. This quantity is simply related to the work of adhesion,[5] $W_{fs}$, between solid and polymer:

$$W_{fs} = \gamma_f + (\gamma_s - \gamma_{fs}) \tag{1}$$

Adhesion tension is also related to the spreading coefficient[5] of the polymer melt on pure solid s

$$S_{f/s} = (\gamma_s - \gamma_{fs}) - \gamma_f \tag{2}$$

Finally, adhesion tension is intimately related to the equilibrium contact angle $\theta$ formed by the polymer melt on the solid. For a system with $S_{f/s} < 0 < W_{fs}$ (polymer melt adheres to, but does not spread on, solid surface), Young's equation[5] gives

$$\gamma_f \cos\theta = \gamma_s - \gamma_{fs} \tag{3}$$

In eq 3, the presence of any vapor that may adsorb on the solid surface, thus modifying its surface tension, is neglected. In other words, the "equilibrium film pressure"[5] is taken as zero. The angle $\theta$ can be thought of as a contact angle in vacuo, formed between a perfectly involatile polymer and a perfectly clean, smooth solid surface.

Adhesion tension at 30 °C is plotted as a function of the strength of segment/solid interactions in Figure 1. A wide range of adsorbing strengths (10 K $< T_s^* <$ 600 K) is considered. The surface tension of our model 50-unit PDMS is $\gamma_f = 14.19$ mN/m (ref 1, Table II). All results were obtained by Newton–Raphson solution of the nonlinear system of interfacial model equations, using analytical derivatives. A zero-order continuation scheme in the parameter $T_s^*$ was implemented, starting from $T_s^* =$ 600 K and progressively lowering $T_s^*$ in steps of 5 K. The convergence characteristics of the numerical solution in the solid/polymer case were significantly better than in the free polymer surface case, discussed in ref 1.

For $T_s^* > 216.45$ K, the spreading coefficient $S_{f/s}$ (eq 2) is positive. A drop of polymer placed on a clean solid surface of finite dimensions will spontaneously spread to form a film covering the surface. (In making this statement, we assume that the quantity of polymer is sufficient to form a film of thickness much larger than chain dimensions.) In the range 13.89 K $< T_s^* <$ 216.45 K, the polymer forms a finite equilibrium contact angle on the solid surface. This angle is larger than 90° (wetting case) for $T_s^* >$ 122.35 K and smaller than 90° (nonwetting case) for $T_s^* <$ 122.35 K. Note that for 13.89 K $< T_s^* <$ 122.35 K adhesion tension is negative, but the work of adhesion (eq 1) is still positive. At $T_s^* = 13.89$ K, the work of adhesion drops to zero, and the contact angle becomes 180°. For values of $T_s^* <$ 13.89 K, a system of two macroscopic phases of polymer and solid adhering to each other is thermodynamically metastable. Intervention of a gaseous film between these two phases would lead to a more stable situation. In other words, molecular contact between solid and polymer phases would be destroyed spontaneously, and adhesion cannot exist. This physical fact is characteristically borne out in the numerical behavior of our interfacial model. Continuation of the solution is impossible below $T_s^* = 10$ K; this indicates that a limit point exists in the vicinity of $T_s^* = 10$ K. For $T_s^* <$ 10 K, one must necessarily "jump", through a "detachment phase transition", to a different, more stable branch of solutions, which consist of a bare solid and a free polymer surface.

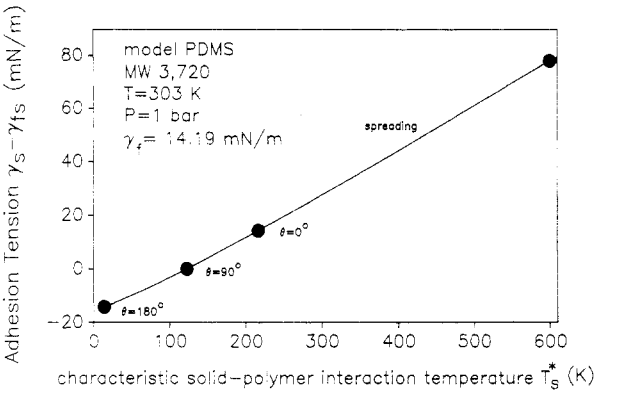


**Figure 1.** Solid/polymer adhesion tension $\gamma_s - \gamma_{fs}$ as a function of the strength of segment/solid interactions, $T_s^*$, for a 50-unit PDMS deposited on various smooth solid surfaces.

In a constant-density lattice modeling approach, a strictly linear relationship between adhesion tension and the energy of segment–solid interactions is predicted.[6] This is because equilibrium structure in a fully occupied lattice polymer is independent of the strength of these interactions and determined solely by entropic factors. On the contrary, the variable-density approach employed here can capture changes in surface structure induced by modifying the adsorption energy of segments. As shown in Figure 1, adhesion tension is, to a good approximation, a linear function of $T_s^*$ on very strongly adsorbing solid surfaces ($T_s^* >$ 400 K); we anticipate that surface structure will be insensitive to $T_s^*$ in this region. On the contrary, a nonlinearity (concavity) in the relation between $\gamma_s - \gamma_{fs}$ and $T_s^*$ develops in the region where adhesive and cohesive forces are comparable in magnitude. This nonlinearity becomes more pronounced with decreasing $T_s^*$. It indicates that one can alter surface structural features considerably by tuning the (relatively weak) segment–solid interaction. In the following, we will concentrate on four representative smooth solid/PDMS interfaces, denoted by the black dots in Figure 1. The first one, at $T_s^* = 600$ K, is characterized by an adhesion tension of 78.02 mN/m. This is comparable to the adhesion tension of ethanol on silica, reported[7] as 110 mN/m. Thus, the value $T_s^* = 600$ K is representative of a "high-energy" solid. The second solid/PDMS interface we will examine is characterized by $T_s^* = 216.5$ K and an adhesion tension of 14.18 mN/m,

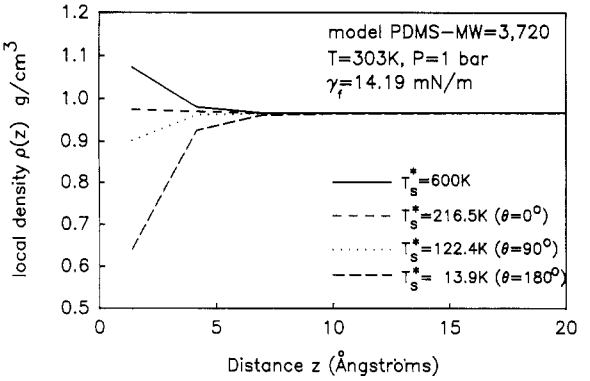


**Figure 2.** Polymer density distributions at interfaces between a 50-unit PDMS liquid and smooth solids of various adsorbing strengths at 30 °C. The equilibrium contact angles are given in parentheses.

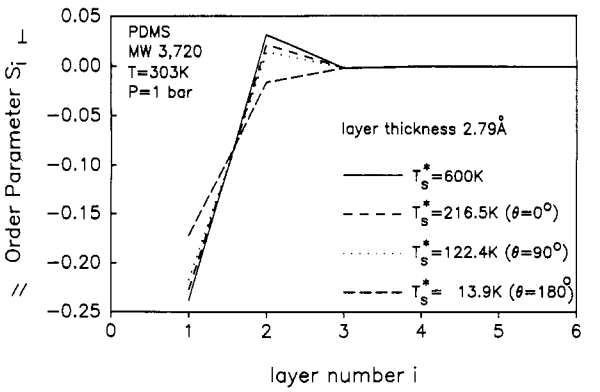


**Figure 3.** Distribution of bond orientation at interfaces between a 50-unit PDMS liquid and smooth solids of various adsorbing strengths at 30 °C. Perfect parallelism of bonds to the solid surface within a layer would correspond to $S_i = -0.50$. Perfect perpendicularity to the surface would correspond to $S_i = 1$.

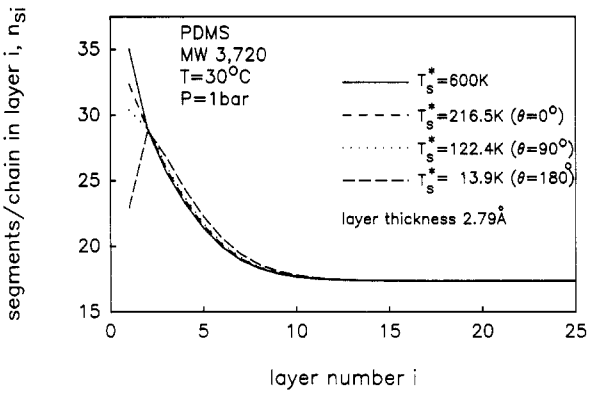


**Figure 4.** Chain shape profiles at interfaces between a 50-unit PDMS liquid and smooth solids of various adsorbing strengths, at 30 °C. The quantity $n_{si}$ stands for the average number of segments that a chain passing through layer $i$ occupies in that layer.

practically equal to the surface tension of the model polymer (equilibrium contact angle $\theta = 0°$). The third solid/PDMS interface is characterized by $T_s^* = 122.35$ K and an adhesion tension of 0 ($\theta = 90°$). The fourth solid/PDMS interface we will examine has $T_s^* = 13.89$ K and an adhesion tension $\gamma_s - \gamma_{fs} = -14.19$ mN/m $= -\gamma_f$. The polymer here is on the verge of spontaneously detaching itself from the solid ($\theta = 180°$).

**Density Distribution.** The local density (or singlet distribution function) of a simple liquid in the vicinity of a smooth, impenetrable solid surface exhibits an oscillatory behavior. This has been demonstrated by both computer simulations[8,9] and surface force measurements.[10] Recent experimental work on the forces exerted between mica surfaces immersed in a polymeric liquid[11] indicates that such oscillations in local density, with period commensurate to the segment diameter, may exist in solid/polymer interfaces, as well. Due to its artificial discretization into layers, our lattice model cannot capture such fine structure effects. It can, however, provide information on local density, averaged over regions large enough that $\rho(z)$ appears as a smooth function. The density obtained with the lattice model clearly shows whether segments are locally concentrated more or less than in the unconstrained bulk.

Density distributions for PDMS at 30 °C, on each of the four smooth solid surfaces mentioned above, are displayed in Figure 2. Near the high-energy surface ($T_s^* = 600$ K), density is enhanced; the strong pulling action of the solid on chain segments overcomes the tendency of chains to move away from the surface due to entropic constraints on conformation. The density distribution is almost flat (actually, slightly enhanced near the solid) in the case of perfect wetting ($T_s^* = 216.45$ K). The region adjacent to the solid is depleted of chain segments in the $\theta = 90°$ case ($T_s^* = 122.35$ K). This depletion becomes dramatic as the limit of adhesion ($T_s^* = 13.89$ K, $\theta = 180°$) is approached. Note that the density profile is much more sensitive to the value of $T_s^*$ in the low-$T_s^*$ (weak adsorption) domain than in the high-$T_s^*$ (strong adsorption) domain. Also note that the density profile in the polymer that is about to detach itself from the solid ($T_s^* = 13.9$ K) starts resembling the rising portion of the free surface profile (ref 1, Figure 7b), which it will assume after detachment. In a way, failure of adhesion is accompanied by a parallel translation of this profile away from the solid surface.

**Bond Orientation.** The distribution of bond orientations in the vicinity of the four solid surfaces of interest is displayed in Figure 3. The bond order parameter, $S_i$, introduced in ref 6 and 1, is used to characterize bond orientation in each layer. Bond orientation profiles at interfaces with $T_s^* = 600$ K, $T_s^* = 216.45$ K, and $T_s^* = 122.35$ K are very similar. A distinct tendency of bonds to lie parallel to the adsorbing surface is observed in the first layer. The prevalent orientation alternates between parallel and perpendicular in successive layers. Orientation effects quickly die out; the absolute value of $S_i$ drops by roughly 1 order of magnitude as one moves from layer to layer. All these characteristics were observed with a simpler, constant-density model of the polymer/solid interface.[6] In fact, the $S_i$ profiles obtained here for the three highest values of $T_s^*$ are quantitatively very close to the corresponding constant-density model profile. Clearly, the alternation of bond orientations discussed in ref 6 is not an artifact of the constant-density assumption, since it persists in the variable-density model.

For $T_s^* = 13.89$ K, the bond orientation profile is considerably different. The oscillation between parallel and perpendicular orientations has subsided. The prevalent orientation is parallel to the solid throughout the interfacial region. Immediately adjacent to the surface, however, the parallel orientation tendency is considerably less intense than in the case of the strongly adsorbing solids. This behavior of $S_i$ is again reminiscent of what happens at a free PDMS surface within the region of appreciable density (compare with Figure 8b of ref 1, beyond layer 5).

**Chain Shape.** The average width[1,6] of chains passing through layer $i$ is plotted against the layer number $i$ in Figure 4, for the four solid/PDMS systems of interest. Pronounced flattening of conformations is observed near the strongly adsorbing solids; the average width $n_{si}$ decays

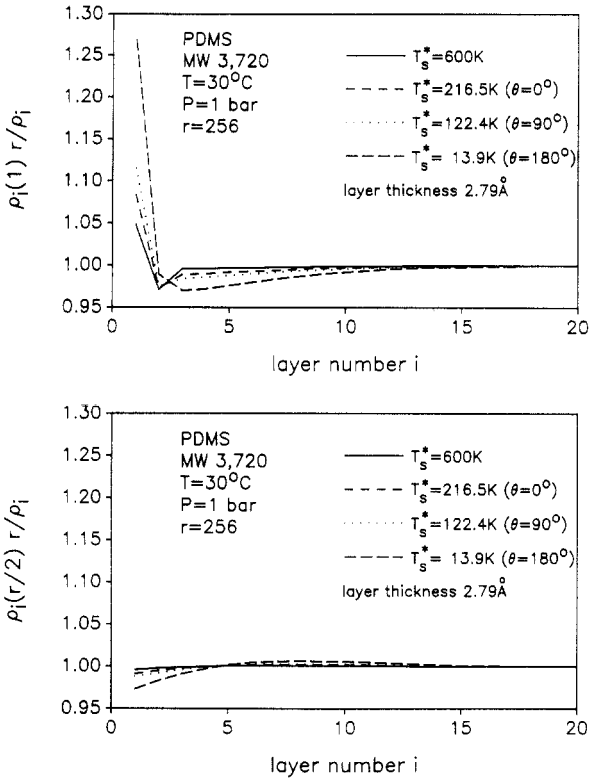


**Figure 5.** (a) Spatial distribution of chain ends at interfaces between a PDMS liquid and four smooth solids of various adsorbing strengths, at 30 °C. (b) Spatial distribution of middle segments at the same interfaces.

monotonically with increasing distance from the surface, down to its unperturbed value. The profiles obtained for $T_s^*$ = 600 K, $T_s^*$ = 216.45 K, and $T_s^*$ = 122.36 K are quite similar. They differ mainly in the first layer; here, the stronger the segment/solid interaction, the flatter the average shape of chains. Again, the flattened profiles predicted by the variable-density model are in close agreement with corresponding results of the constant-density model.[6] Only in the case of the very weakly adsorbing solid ($T_s^*$ = 13.98 K) is some narrowing of conformations observed adjacent to the surface, relative to the region further in the polymer. Again, one recognizes in the chain shape profile corresponding to $\theta$ = 180° some seeds of free surface structure (compare with Figure 9b of ref 1).

**Distribution of Chain Ends and Middle Segments.** The spatial distribution of chain ends and middle segments in our model polymer/solid interfaces is examined in Figure 5, along the lines discussed in ref 1. The concentration of ends is enhanced in the first layer, and this enhancement is greater the lower the value of $T_s^*$. Accordingly, subsequent layers are depleted of end segments. The surface enhancement in end segments, however, is much weaker than in the case of the highly attenuated free polymer surface (compare with Figure 10b of ref 1). The concentration profile of middle segments departs only little from uniformity. Profiles for $T_s^*$ = 13.89 K show some qualitative differences from the three higher $T_s^*$ profiles.

As discussed in ref 1, the distribution of chain tails in the interfacial region is affected by both energy and entropy effects. In the free surface case, the top layers of the lattice have a very low density. The tendency to maximize cohesive energy and the tendency to minimize conformational restrictions work in the same direction, leading to a dramatic enrichment of the surface region in tails. In the solid/polymer case, variations in density are weaker. Near a high-energy surface ($T_s^*$ = 600 K), the density profile is actually inverted with respect to the free surface case. As a result, energy and entropy factors affecting the position of end segments now compete, rather than cooperate. A balance is struck at a spatial distribution of ends that does not depart much from uniformity.

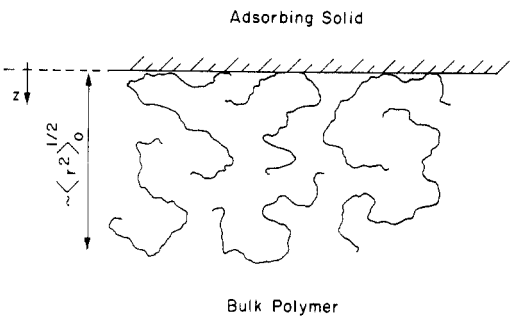


**Figure 6.** Pictorial representation of the molecular structure of a polymer melt near a strongly adsorbing, smooth solid surface.

In Figure 6, we have attempted to sketch the structure of a polymer melt in the vicinity of a strongly adsorbing surface, as it emerges from the features discussed above. Chains are flattened and densely packed adjacent to the solid. Conformation gradually relaxes to its unperturbed characteristics, as one moves away toward the bulk.

## 3. Polymer Films Confined between Solid Surfaces Immersed in Macromolecular Liquids at Small Distances

**The Problem.** The development of the surface force apparatus[10] has made it possible to measure "solvation forces", exerted between solid surfaces of macroscopic dimensions and separated by fluid films of thickness on the order 10–1000 Å. Typically, two mica surfaces are used in a crossed cylinder geometry. The surfaces are practically molecularly smooth. Forces between them have been measured in low molecular weight liquids consisting of roughly spherical molecules,[12] and in polymer solutions,[13] as well as in solutions of block copolymers.[14] Very recently, surface force measurements have been performed in neat (no solvent) macromolecular fluids.

Static forces between crossed cylindrical mica surfaces immersed in even-numbered *n*-alkanes from hexane to hexadecane were presented by Christenson et al.[15] In these liquids, the force law consists of a decaying oscillatory function of distance, superimposed on a weakly attractive background. The period of the oscillations is approximately 5 Å, commensurate with the diameter of an alkane chain, for all chain lengths examined. The attractive background, on the order of $F_c/R_c$ = 1 mN/m, can be accounted for by a continuum consideration of van der Waals forces (Lifschitz theory).

Measurements on mica surfaces separated by a drop of polydiperse poly(dimethylsiloxane), with a number-average degree of polymerization of approximately 50, have been performed by Horn and Israelachvili.[11] Oscillations, of a period commensurate to the chain diameter, are also observed in this case. In striking contrast to the alkane case, however, these are superimposed on a strongly *repulsive* background, on the order of $F_c/R_c$ = 10–100 mN/m. More recently, Israelachvili and Kott[16] performed the same measurement on pure, monodisperse polybutadienes of approximate degrees of polymerization 20 ($\langle s^2\rangle_0^{1/2}$ = 11.5 Å) and 65 ($\langle s^2\rangle_0^{1/2}$ = 21.5 Å). Again, strongly repulsive forces on the order of 10 mN/m were observed upon approaching the mica surfaces. The distance dependence of the repulsive force was quasi-exponential at separations larger than 70 Å. At very small distances, repulsive forces increased very steeply, suggesting the occurrence of a "hard

wall" at $h \simeq 30$ Å ($2.6\langle s^2\rangle_0^{1/2}$) and at $h \simeq 50$ Å ($2.3\langle s^2\rangle_0^{1/2}$) for the lower and higher molecular weight samples, respectively. No oscillations were observed in the polybutadiene case.

A thorough examination of static surface forces in a perfluorinated polyether of number-average molecular weight 8800 ($\langle s^2\rangle_0^{1/2} = 26$ Å) and polydispersity index 1.70 is presented by Montfort and Hatziioannou. Chemically, the sample was a statistical copolymer of fluoroethylene oxide (60%) and fluoromethylene oxide (40%) units. Immersing the mica surfaces in liquid polymer and using a droplet of polymer between the surfaces in a dry inert atmosphere led to identical results. Again, a repulsive, nonoscillatory force law was observed. The force decays slowly at large separations, extending out to distances as large as 800 Å ($30\langle s^2\rangle_0^{1/2}$). A strong repulsive wall is approached at a separation of roughly 100 Å ($3.85\langle s^2\rangle_0^{1/2}$).

The above intriguing experimental observations call for an explanation at the molecular level. Very little theoretical work has been done on the problem of surface forces in macromolecular liquids at very small separations. A mean field theory, based on the rotational isomeric state model, developed for normal alkanes[15] was unsuccessful in predicting experimental observations. Although it invokes a realistic representation of chain geometry, this theory arbitrarily assumes a uniform distribution of chain ends in the interfacial region, does not take into account the effects of intermolecular interactions on chain conformation, and completely neglects adsorptive segment–surface interactions. It is essentially a single-chain theory and thus not necessarily applicable to the highly inhomogeneous polymer film phase encountered in the surface force apparatus. A simple and elegant lattice treatment of very thin polymer films was developed in a research report by Barker, which predates the surface measurements on polymers.[18] Full occupancy of the lattice by chain segments is assumed, and a Flory-type random mixing approximation is used in the entire film to account for excluded volume effects. No equilibrium between the film and a bulk polymer phase is assumed. Also, no condition of internal equilibration is imposed within the film (i.e., it is not required that all chains have the same chemical potential). A repulsive surface force, that rises sharply with decreasing distance, is predicted.

de Gennes[19] has recently given some consideration to the interactions between two plates separated by a film of molten polymer. He argues that, under conditions of complete thermodynamic equilibrium, the polymer should not give rise to any forces between the plates. As a possible explanation of the repulsive forces actually observed, he proposes that the chains in direct contact with the solid are "pinned", or "anchored", irreversibly on the surfaces. Upon approaching the surfaces, one gets steric repulsion similar to that observed with surface-grafted chains in solution.

In this section, we apply our variable-density lattice model to a liquid polymer confined between two closely spaced solid surfaces, in order to predict surface forces and structural features expected at equilibrium. The reader should interpret results reported here in the light of two *caveats*: First, we are using a mean field theory to treat a very thin phase, in which packing should depend sensitively on the details of molecular geometry; results are expected to be only approximate, especially at separations so small as to be commensurate with individual segment dimensions.[20] Second, as a result of its discrete, layerwise nature, the model cannot predict oscillating "structural" forces, due to segmental organization near the solid surfaces, even if such forces exist in reality. It can only predict the central, attractive or repulsive trend in the force, on which such oscillations would be superimposed.

**Thermodynamics of the Surface Force.** Consider two flat solid plates, each of area $\hat{a}$, separated by a distance $h$, and immersed in an infinite reservoir of macromolecular liquid at temperature $T$ and pressure $P_b$ (ref 1, Figure 1). We will assume here that $h \ll \hat{a}^{1/2}$, so that the plates can be treated as inifinite in extent. To keep the plates in place, an external force must, in general, be applied on each of them via a spring or solid support; this is the force actually measured in a surface force apparatus. A positive $F$ corresponds to "repulsion" and a negative $F$ to "attraction" between the plates.

An expression for $F$ can be arrived at via a thermodynamic analysis of a reversible change of the system, which brings the plates closer by d$h$. The details of this analysis will not be presented here. The result is

$$F = -\frac{\mathrm{d}[n_f(\Upsilon_f - \Upsilon_b)]}{\mathrm{d}h}$$

$$F'' \equiv \frac{F}{\hat{a}} = -\frac{\mathrm{d}}{\mathrm{d}h}\left[\frac{n_f}{\hat{a}}(\Upsilon_f - \Upsilon_b)\right] \tag{4}$$

Equation 4 permits obtaining the surface force from a knowledge of the amount of polymer between the plates and of the molar availabilities of the interfacial and bulk polymer phases. Both $n_f$ and $\Upsilon_f$ are functions of $h$.

If the film thickness is large, the quantity $n_f(\Upsilon_f - \Upsilon_b)$ is directly related to the "adhesion tension" $\gamma_s - \gamma_{fs}$ between the polymer and the solid (ref 1, eq 17), and eq 4 can be rewritten as

$$F'' = \frac{F}{\hat{a}} = -2\frac{\partial(\gamma_{fs} - \gamma_s)}{\partial h}\bigg|_{P_b,T} \equiv -2\frac{\partial \gamma_{fs}}{\partial h}\bigg|_{T,G_b} \tag{5}$$

Equation 5 has been given by Ash, Everett, and Radke[21] and by Magda, Tirrell, and Davis.[9]

The quantity $(n_f/\hat{a})(\Upsilon_f - \Upsilon_b)$ has been obtained in the context of the interfacial theory outlined in ref 1. Assuming full thermodynamic equilibrium between the film and bulk phases

$$\frac{n_f}{\hat{a}}(\Upsilon_f - \Upsilon_b) = \frac{2kT}{(v^*/N_L)^{2/3}}\left\{\sum_{i=1}^{m}\left[\left(1 - \frac{1}{r}\right)\varphi_i + \ln(1 - \varphi_i) + \left(\frac{T^*}{T}\right)\varphi_i\langle\varphi_i\rangle\right] + m\left(\frac{P_b v^*}{RT}\right)\right\} \tag{6}$$

More interesting than a pair of flat, parallel solid plates is a system of two convex, cylindrical surfaces at right angles to each other. This geometry is invariably used in the actual surface force measurements, due to its experimental advantages.[10-17] In interpreting results, the system of two crossed cylindrical surfaces of radius $R_c$ is taken as equivalent to that of a plane and a spherical surface of radius $R_c$ at the same minimal separation $h$. The plane/sphere geometry can, in turn, be related to the plane/plane geometry via the Derjaguin approximation. The quantity $F_c(h)/R_c$, where $F_c$ is the force in the plane/sphere case, is expressed in terms of the interaction energy per unit area, $E''(h)$, in the plane/plane geometry, as follows:[22]

$$\frac{F_c(h)}{R_c} = 2\pi E''(h) \tag{7}$$

The derivation of eq 7 is based on envisioning the spherical surface as an assembly of small, locally flat surfaces. In the surface force apparatus, $R_c$ is much larger than the separation $h$ and also much larger than typical chain di-

mensions; the mica surfaces would indeed appear to the polymer as locally flat.

The interaction energy $E''(h)$ is equal to the work produced by the surface forces, if the plates are taken from a separation $h$ to infinite separation, at which they no longer interact. By use of eq 4

$$E''(h) = \int_h^\infty F''(z)\,dz = \int_h^\infty \left\{-\frac{d}{dz}\left[\frac{n_f}{\hat{a}}(\Upsilon_f - \Upsilon_b)\right]\right\} dz = \left[\frac{n_f}{\hat{a}}(\Upsilon_f - \Upsilon_b)\right]_h - \left[\frac{n_f}{\hat{a}}(\Upsilon_f - \Upsilon_b)\right]_\infty \quad (8)$$

An early form of eq 8 has been derived by Mackor and van der Waals.[23] Combining eq 7 and 8 yields

$$\frac{F_c(h)}{R_c} = 2\pi\left\{\left[\frac{n_f}{\hat{a}}(\Upsilon_f - \Upsilon_b)\right]_h - \left[\frac{n_f}{\hat{a}}(\Upsilon_f - \Upsilon_b)_\infty\right]\right\} \quad (9)$$

which permits obtaining the force in the curved geometry from the molecular characteristics of the system, through eq 6.

**Surface Force Results.** All calculations reported in this paper were performed with the monodisperse model "sample" of poly(dimethylsiloxane) studied in section 2 at an ambient temperature of $T$ = 303 K and pressure of $P_b$ = 1 bar. Again four solids were considered, characterized by $T_s$* values of 600, 216.45, 122.35, and 13.89 K. Among these, the $T_s$* = 600 K solid is closest to the mica used in surface force experiments. As will be seen from subsequently reported results, the $T_s$* = 13.89 K system, and even the $T_s$* = 122.35 K system for all but the smallest separations, are metastable. In reality, the polymer film in these systems would spontaneously break, giving way to a more stable state, whereby all polymer exists in the unconstrained bulk form and vacuum occupies the space between the solid surfaces. Thus, the $T_s$* = 600 K and $T_s$* = 216.45 K systems are the most physically relevant among the four examined here.

The set of interfacial model equations[1] was solved for PDMS films of various thicknesses, sandwiched between smooth, flat solid plates of each of the above four chemical constitutions. For each system studied, the plate separation was initially taken as $2m$ = 40 lattice layers ($h$ = 111.7 Å). The half-spacing $m$ was progressively reduced in intervals of one lattice layer, down to a final plate separation of $2m$ = 2 lattice layers ($h$ = 5.6 Å). A second-order continuation scheme in the parameter $m$ was implemented to achieve convergence at low separations.

Surface forces in the flat plate geometry were computed via eq 4 and 6. The derivative with respect to separation in eq 4 was calculated by finite differences between results at successive $h$ values. Surface forces in a crossed cylinder geometry were obtained from flat plate results via eq 9. The availability per unit area at infinite separation, referred to the bulk, $[(n_f/\hat{a})(\Upsilon_f - \Upsilon_b)]_\infty$, was obtained from a calculation at $2m$ = 200 layers. Results were found to be completely insensitive to h beyond this distance, which is thus taken as representative of "infinite separation".

Results on the force per unit area, $F/\hat{a}$, exerted between two flat surfaces immersed in 50-unit PDMS, are plotted in Figure 7a. The four different solids discussed above are considered. The force-to-radius ratio, $F_c/R_c$, in the crossed cylinder geometry, is presented as a function of separation in Figure 7b.

Predicted forces are repulsive at separations larger than $\langle s^2\rangle_0^{1/2}$ in all cases. The magnitude of the repulsion increases with decreasing distance. In the flat plate geometry, interactions are insignificant beyond a separation of

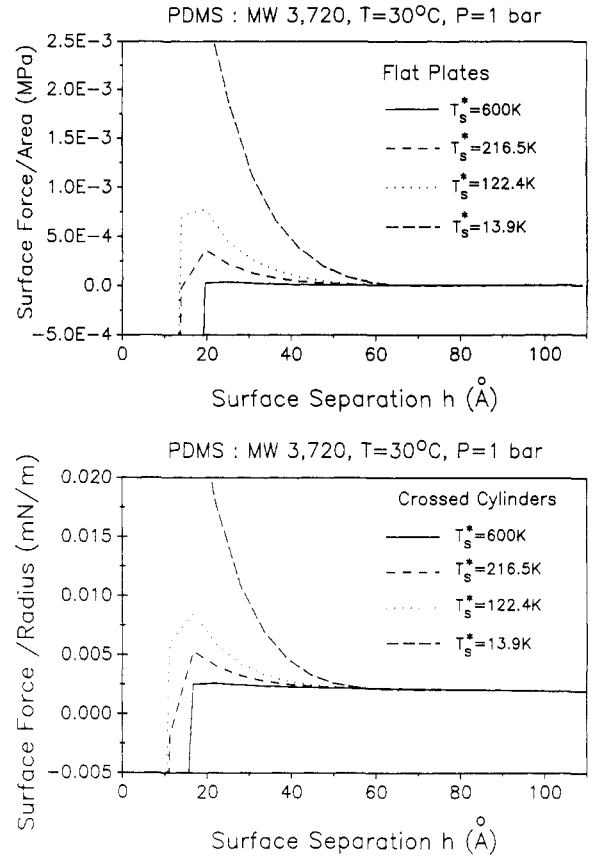


**Figure 7.** (a) Force per unit surface, $F/\hat{a}$, between two smooth, flat solid plates immersed in a poly(dimethylsiloxane) liquid of degree of polymerization 50. (b) Force divided by radius, $F_c/R_c$, for a pair of smooth, cylindrical solid surfaces at right angles to each other, immersed in the same polymer. Solids of four different adsorbing strengths $T_s$* are considered.

70 Å, or approximately $4\langle s^2\rangle_0^{1/2}$. In the crossed cylinder system, there is a weak long-range component of the force that decays very slowly with increasing separation; this long-range tail results from integrating the flat plate forces of Figure 7a out to infinite separation. In the actual measurement, this weak background would be indistinguishable from zero.

In the three stronger adsorbing cases ($T_s$* ≥ 122.35 K), our equilibrium model predicts that a significant adhesive force will develop at separations smaller than $\langle s^2\rangle_0^{1/2}$ due to extensive bridging by highly confined polymer chains adsorbed on both surfaces. The curves of Figure 7b drop precipitously to values of −4.29 mN/m ($T_s$* = 600 K), −1.22 mN/m ($T_s$* = 216.45 K), and −0.96 mN/m ($T_s$* = 122.35 K) at $h$ = 5.6 Å. In the very weakly adsorbing case, $T_s$* = 13.89 K repulsive interactions rise very steeply to 0.90 mN/m at a separation of $h$ = 11.2 Å, below which it is impossible to maintain even a metastable film of appreciable density between the plates (i.e., cavitation inevitably occurs.) These small $h$ results should, of course, be interpreted in the light of the *caveats* stated in the beginning of section 3.

The repulsive forces active at separations of $\langle s^2\rangle_0^{1/2}$ to $4\langle s^2\rangle_0^{1/2}$ between strongly adsorbing surfaces are very weak. At a given separation $h$, the better the adhesion between polymer and solid, the smaller the surface force. Thus, in the case of the high-energy $T_s$* = 600 K surfaces, which are most representative of the mica used in actual experiments, repulsive forces are truly negligible; they go through a maximum of only 2.6 μN/m at $h$ = 22.3 Å.

**Film Structure.** It is interesting to examine how the microscopic structure of the polymer film depends on the

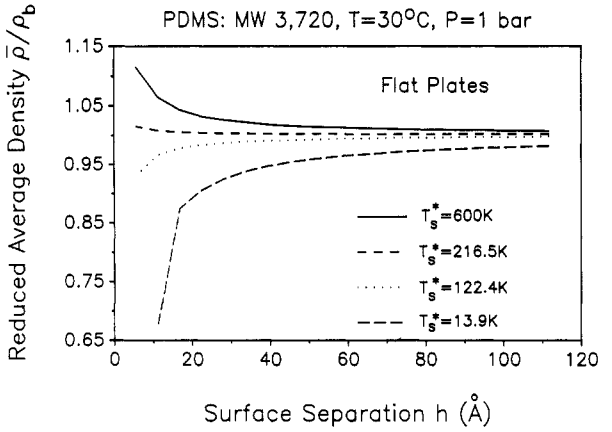


**Figure 8.** Average density of a thin PDMS film confined between two flat solid plates as a function of plate separation. Full equilibrium between the film and the surrounding unconstrained bulk polymer is assumed. Densities have been reduced by the bulk polymer density $\rho_b = 0.965$ g/cm$^3$. Results are presented for four solid surfaces, characterized by $T_s^* = 600$, 216.45, 122.35, and 13.89 K.

separation and on the chemical nature of the solid surfaces that confine it. All results reported here refer to the flat plate geometry; they can be ported to crossed cylinders, on the assumption that these behave locally as flat plates.

Decreasing the plate separation was found to bring about an essentially rigid inward translation of the polymer density profile. In the middle region between the plates, the polymer invariably assumes its bulk density. The extent of this middle region, in which density profiles are flat, is reduced as plates are brought together. Other than that, however, density profiles in each half of the polymer film are almost insensitive to plate separation, for all $T_s^*$ values studied; they are practically indistinguishable from the corresponding single interface profiles, plotted in Figure 2. Under the full equilibrium requirement, chains always manage to arrange themselves so as to conserve the distribution of segment density near each surface. Only at very small separations, when the two profiles interpenetrate significantly, are some subtle deviations in the density profiles observed, and these lead to the development of the weak repulsive forces of Figure 7. The forces are greatest in the case of the $T_s^* = 13.89$ K surface, because here the thickness of the "boundary layer" region, over which density departs from its bulk value, is greatest (compare Figure 2).

The *average* film density, $\bar{\rho}$, defined as the total mass of polymer in the gap over the total volume of the gap, is presented as a function of plate separation in Figure 8, for the four solids considered. The ordinate is obtained straightforwardly as

$$\frac{\bar{\rho}}{\rho_b} = \frac{1}{m\varphi_b}\sum_{i=1}^{m}\varphi_i \qquad (10)$$

The changes in average film density depicted in Figure 8 stem mainly from the fact that, as the two plates are brought together, the flat portion of the density profile narrows down, and the two "boundary layers" on the plates become more and more dominant. An enhancement of the average density is observed, therefore, for $T_s^* = 600$ and 216.45 K, whereas a depletion develops for $T_s^* = 122.35$ K and $T_s^* = 13.89$ K, as expected from the profiles of Figure 2. The departure of density from its bulk value is particularly pronounced in the case of the $T_s^* = 13.9$ K system.

An examination of chain conformations in the interfacial region revealed that macromolecules become more and more flattened as the plates approach each other. The occurrence of this flattening in the surface layer indicates that, as plates are brought together, some chains desorb, offering the sites they occupy to other adsorbed chains or to tails and loops of chains adsorbed on the opposite plate; this partial displacement of adsorbed chains occurs under preservation of the local density.

## 4. Discussion

We have presented some results, obtained by applying a variable-density mean field lattice model to interfaces between a bulk liquid polymer phase and smooth solids of various adsorbing strengths. With this model, it is possible to connect the equilibrium wetting and spreading behavior of polymer melts on solids to fundamental molecular information on chain chemistry and polymer segment/solid interactions. The model provides a detailed picture of structure in the vicinity of the solid surface, which is distinctly different from that at a free polymer surface. Near a strongly adsorbing smooth solid surface, chains are pronouncedly flattened and densely packed. Their average width drops monotonically to its unperturbed value as one moves away from the solid, over a distance roughly equal to the end-to-end length. Subtle changes in density and local structure are observed upon varying the strength of segment/solid interactions; these changes become more expressed in the case of weakly adsorbing solids.

We have also developed an approach for predicting the structure of and forces exerted due to very thin polymer films, confined between smooth solid surfaces immersed in macromolecular liquids at small distances. Our approach assumes that the confined film is fully equilibrated with the surrounding unconstrained melt, with respect to exchange of work, heat, and mass. Our model predicts *negligible* "long-range" surface forces for the case of strongly adsorbing solid surfaces, such as mica. This result confirms de Gennes' statement that there should be no forces due to a film of melt at full thermodynamic equilibrium.[19] In practice, the very weakly repulsive forces (on the order of 1 $\mu$N/m) predicted by the full equilibrium model at separations of 1–4 unperturbed radii of gyration would be overshadowed by the long-range attractive van der Waals interactions between the plates. Thus, our results are consistent with recent experimental measurements on liquid normal alkanes;[15] no evidence of a repulsive surface force, due to the chain molecules, was reported for these systems.

Long-range repulsive forces of the magnitude reported in the case of poly(dimethylsiloxane),[11] polybutadiene,[16] and perfluorinated polyether[17] are not predicted by our model. This suggests that some departure from equilibrium is required for such forces to appear. In practice, surface force measurements are performed by introducing a sequence of stepwise changes in the configuration of the springs of the apparatus that result in successive reductions of the interplate separation. Each time the springs are displaced, the film must reequilibrate with the surrounding bulk; it must expel some chains into the bulk, and reorganize itself, so that the chemical potential of chains in the remaining film phase is again everywhere the same and equal to the chemical potential of chains in the bulk phase. Differences in chemical potential are effaced slowly, by chain diffusion. It is conceivable that the time devoted to the measurement between successive changes in the configuration of the springs is insufficient for complete equilibration to occur. A repulsive force of hydrodynamic origin would then be measured. If this interpretation is correct, the long diffusion time of chains or, equivalently,

the high viscosity of polymer melts is at least as important as their macromolecular nature in giving rise to repulsive interactions. The striking difference in reported surface force behavior between hydrocarbons and longer chain polymers may be due to their widely disparate viscosities. Indeed, very recent results of Horn et al.[24] indicate that long-range repulsive forces subside when the film is allowed more time to equilibrate between successive reductions of the interplate distance and that previously reported repulsive forces can be explained on hydrodynamic grounds.

If a departure from thermodynamic equilibrium is responsible for long-range repulsive forces, different forces could be observed at the same separation, depending on the sequence in which the surface force measurements are taken. Such "hysteresis" effects have actually been observed with 65-unit polybutadiene by Israelachvili and Kott;[16] they provide support to the hypothesis that the system in actual experiments is not in full thermodynamic equilibrium. Interestingly, previous modeling considerations by Barker,[18] which led to the prediction of repulsive forces, invoked a picture of incomplete equilibration: although characterized by constant density, Barker's lattice polymer film is not in contact with bulk polymer in any way; also, no condition of internal equilibration, such as the one used in this work (chemical potential of all conformations the same), was imposed on the film.

All surface measurements with polymers, including the most recent ones,[24] indicate that a steep repulsive "wall" is approached at separations commensurate with $2\langle s^2\rangle_0^{1/2}$. Our lattice model does not predict such a wall in the case of a high-energy surface (Figure 7b). A scenario that can possibly explain this repulsive wall has been proposed by de Gennes.[19] According to this scenario, chains in direct contact with the solid surfaces are "pinned" or "anchored" on them. As surfaces are approached, the free parts of "pinned" chains give rise to steric repulsions, analogous to those observed in solution with surface-grafted polymers or diblock copolymers. Note that this interpretation also involves a departure from full equilibrium: the "pinning" or immobilization of segments on the surface amounts to an inhibition of lateral diffusion of adsorbed chains. Thus, adsorbed chains and free chains are not truly equilibrated. Recent dynamic Monte Carlo simulations[25] indicate that the self-diffusion of chains adjacent to a high-energy solid wall is severely hindered in comparison to the bulk. Thus, an interpretation of the repulsive "wall" at $h \simeq 2\langle s^2\rangle_0^{1/2}$ on the basis of "pinning" is plausible.

The present modeling work suggests that some additional experimental measurements would be worth undertaking in the surface force apparatus. First, it would be interesting to study the effects of polymer/solid adhesion on surface forces. This could be done by examining a given polymer between a series of mica plates, surface-modified in various ways in order to enhance or suppress chain adhesion, or by examining a series of polymers of systematically varying chemical constitution between the same mica plates. Our modeling work suggests that the adhesion tension, a thermodynamic quantity readily obtainable from interfacial tension measurements at a single solid/polymer interface, is very important and should be reported together with surface force curves. Second, it would be very worthwhile to monitor changes in the mean density of the film as the solid surfaces are approached; this could be done spectroscopically. Third, if some process of falling out of equilibrium is responsible for strong repulsion, surface force results should depend on the measurement history (initial plate separation, direction in which separation is varied), on temperature, and on the time scale of the measurements. The existence of such effects should be probed in detail.

On the theoretical level, it would be very desirable to have a model that affords a more realistic representation of actual chain geometry, incorporates long-range segment–segment and segment–surface interactions, and is free of the artificialities of the lattice. The development of such a model, and its application to free polymer surfaces, to bulk polymer/solid interfaces, and to confined polymer films, is one of our immediate objectives.

**Acknowledgment.** We are grateful for financial support from the IBM Corp., under a Shared University Research Program contract, Agreement No. SL 88037. Computational resources were made available through support provided by the Director, Office of Energy Research, Office of Basic Energy Sciences, Materials Science Division of the U.S. Department of Energy under Contract No. DE-AC03-76SF00098. I also thank the National Science Foundation for a Presidential Young Investigator Award, Grant No. DMR-8857659. Illuminating discussions with Dr. Georges Hadziioannou, Dr. Sanat Kumar, Dr. Dominique Ausserrê, Susan Hirz, and Al Ward at IBM are deeply appreciated.

## Symbols[26]

| | |
|---|---|
| $E$ | potential energy of interaction between plates due to polymer film |
| $F$ | surface force exerted between flat plates due to the intervening film of macromolecular liquid, after subtraction of the bulk pressure contribution, $P_b\hat{a}$ |
| $F_c$ | surface force exerted between crossed cylinders due to the intervening film of macromolecular liquid, after subtraction of the bulk pressure contribution |
| $\langle r^2\rangle_0^{1/2}$ | root mean squared unperturbed end-to-end distance |
| $R_c$ | radius of a mica semicylinder |
| $\langle s^2\rangle_0^{1/2}$ | root mean squared unperturbed radius of gyration |
| $S_{f/s}$ | spreading coefficient of polymer on solid surface |
| $W_{fs}$ | work of adhesion between solid and polymer |

## Greek Symbols

| | |
|---|---|
| $\gamma_f$ | surface tension of pure polymer |
| $\gamma_{fs}$ | interfacial tension in polymer/solid system |
| $\gamma_s$ | surface tension of solid |
| $\theta$ | equilibrium contact angle between polymer and solid |
| $\bar{\rho}$ | average density of polymer in interfacial (film) region |

## Superscripts

| | |
|---|---|
| $''$ | per unit area |

## Subscripts

| | |
|---|---|
| c | crossed cylinder geometry |
| fs | solid/polymer interface |
| $\infty$ | infinite plate separation |

## References and Notes

(1) Theodorou, D. N. *Macromolecules*, preceding paper in this issue.
(2) Sanchez, I. C.; Lacombe, R. H. *J. Chem. Phys.* **1976**, *80*, 2352; *Polym. Lett.* **1977**, *15*, 71; *Macromolecules* **1978**, *11*, 1145.
(3) Scheutjens, J. M. H. M.; Fleer, G. J. *J. Phys. Chem.* **1979**, *83*, 1619; **1980**, *84*, 178; *Macromolecules* **1985**, *18*, 1882.
(4) Flory, P. J. *Statistical Mechanics of Chain Molecules*; Interscience: New York, 1969; p 178.
(5) Hiemenz, P. C. *Principles of Colloid and Surface Chemistry*; Marcel Dekker: New York, 1977; Chapter 6.
(6) Theodorou, D. N. *Macromolecules* **1988**, *21*, 1400.
(7) Van Voorhis, J. J.; Craig, R. G.; Bartell, F. E. *J. Chem. Phys.* **1957**, *61*, 1513.
(8) Snook, I. K.; Van Megen, W. *J. Chem. Phys.* **1980**, *72*, 2907.
(9) Magda, J. J.; Tirrell, M. V.; Davis, H. T. *J. Chem. Phys.* **1985**, *83*, 1888.
(10) Israelachvili, J. N.; Adams, G. E. *J. Chem. Soc., Faraday*

*Trans. 1* **1978**, *74*, 975. Horn, R. G.; Israelachvili, J. N. *J. Chem. Phys.* **1981**, *75*, 1400.
(11) Horn, R. G.; Israelachvili, J. N. *Macromolecules* **1988**, *21*, 2836.
(12) Israelachvili, J. N.; Christenson, H. K. *Physica* **1986**, *140A*, 278.
(13) Israelachvili, J. N.; Tirrell, M.; Klein, J.; Almog, Y. *Macromolecules* **1984**, *17*, 204.
(14) Hadziioannou, G.; Patel, S.; Granick, S.; Tirrell, M. *J. Am. Chem. Soc.* **1986**, *108*, 1869.
(15) Christenson, H. K.; Gruen, D. W. R.; Horn, R. G.; Israelachvili, J. N. *J. Chem. Phys.* **1987**, *87*, 1834.
(16) Israelachvili, J. N.; Kott, S. J. *J. Chem. Phys.* **1988**, *88*, 7162.
(17) Montfort, J. P.; Hadziioannou, G. *J. Chem. Phys.* **1988**, *88*, 7187.
(18) Barker, J. A. IBM Research Report RJ4206 (46284), 1984.
(19) de Gennes, P.-G. *C. R. Acad. Sci.* **1987**, *305*, 1181.
(20) Peterson, B. K.; Gubbins, K. E.; Heffelfinger, G. S.; Marini, U.; Marconi, B.; van Swol, F. *J. Chem. Phys.* **1988**, *88*, 6487.
(21) Ash, S. G.; Everett, D. H.; Radke, C. *J. Chem. Soc., Faraday Trans. 2* **1973**, *69*, 1256.
(22) Israelachvili, J. N. *Intermolecular and Surface Forces*; Academic Press: London, 1985; Chapter 10.
(23) Mackor, E. L.; van der Waals, J. H. *J. Colloid Sci.* **1952**, *7*, 535.
(24) Horn, R. G.; Hirz, S. J.; Hadziioannou, G.; Frank, C. W.; Catala, J. M. *J. Chem. Phys.* **1989**, *90*, 6767.
(25) Mansfield, K. F.; Theodorou, D. N. *Macromolecules* **1989**, *22*, 3143.
(26) The meaning of all symbols not listed here has been explained in the preceding paper in this issue.

# Bilayer Smectic Phases in Polymeric Liquid Crystals with Nonpolar Mesogens

**Edward N. Keller**

*Racah Institute of Physics, Hebrew University, Givat Ram, 91904 Jerusalem, Israel.*
*Received February 9, 1989; Revised Manuscript Received April 14, 1989*

ABSTRACT: Recent experiments have noted the presence of partial bilayer smectic A ($A_d$) liquid-crystal phases in several types of side-chain polymeric liquid crystals, which do not contain highly polar groups in the mesogens. We show that the aromatic rigid core overlap between neighboring mesogens seems to be rather fixed among a wide range of materials, possibly determined by dipolar-induced dipolar forces.

## Introduction

The appearance of bilayer phases for monomeric liquid crystals is innevitably associated with highly polar chemical groups such as the cyano radical.[1] These mesogens are thought to form dimers as a consequence of polar interactions.[2] To our knowledge, no other type of monomeric liquid crystal forms bilayer phases. The situation is different for polymeric liquid crystals. Although the incorporation of polar mesogens forms bilayer phases, as expected, some nonpolar mesogens are known to dimerize[3] and to form bilayers when they are present in side-chain polymeric liquid crystals.[4] It is generally acknowledged that, in these materials, this effect is initialized by the natural alteration of mesogens in an antiparallel ordering (Figure 1a). This ordering does not necessarily produce a bilayer phase, since a layer spacing, $d$, equal to a single mesogen length, $d = l$, is also possible in the case that the mesogens lie completely side by side (see Figure 1b). Since nonpolar monomeric liquid crystals almost invariably show monolayer ($d = l$) orderings (for at least the high-temperature phases), we expect that such ordering should be the rule in side-chain polymeric liquid crystals. Exceptions to this rule, which are surprisingly common (as we will show), point out the existence of forces that are manifested when the mesogens are constrained to the antiparallel orderings of Figure 1. Since such phases have many properties in common with *polar* monomeric liquid crystals,[3] we expect that some type of *polar* forces (acting in conjunction with the polymeric backbone) are important in causing these orderings in at least some polymeric liquid crystals.

## Results and Discussion

The first thorough study of bilayer-forming polysiloxane polymeric liquid crystals was performed at Bordeaux.[4] Subsequent high-resolution X-ray studies[5] of one member of the polymer family studied at Bordeaux (viz., P4.1) showed that the bilayer phase is a true smectic A phase (commonly known as $A_d$, i.e., $l < d < 2l$) with phase-transition properties similar to those of monomeric liquid crystals but having surprisingly large bare correlation lengths (which is also found for some polar monomeric liquid crystals[5]). To understand these materials, we developed a molecular drawing computer program that accurately portrays bond lengths and conformations in these chemicals.[6] Comparison of our program results with X-ray crystallography tables on molecules similar to a typical liquid-crystal mesogen showed that our predictions for molecular lengths were accurate to better than 1 Å. In Figure 2b, we depict the molecular organization of P6.1 (whose mesogens are separately drawn in Figure 2a).[7] In Figure 2b, we have assumed that the distance between silicon atoms of neighboring polymers can be identified with the average layer spacing, $d$, as measured by ref 4 (i.e., ~36.8 Å). The flexible tails are drawn in the all-trans fully extended configuration. (This is consistent with observations that the flexible tail is "melted" at temperatures, $T \gg T_g$,[8] and it will tend to occupy a volume equal to that of a flexible tail in the all-trans fully extended conformation.) The configuration of the core is extrapolated from X-ray crystallography data of a chemically similar species, viz., deoxyanisoin.[9] If we suppose that the core overlap (the core being defined as the atoms including and beyond the oxygen that connects to the $(CH_2)_n$ flexible side chain) is constant for all P$n$.1 compounds, then the interlayer spacing, $d$ (at the same reduced temperature), as a function of $n$ can be written as:

$$d\ (\text{Å}) = 36.8\ \text{Å} + (n - 6)2.5\ \text{Å} \qquad (1)$$

Figure 3 plots eq 1 with the experimentally measured layered spacings, $d$. Excellent agreement is obtained. This highly suggests that the core overlap is constant for all $n$ measured.

It is possible to show that the constant core overlap is not a side effect of a particular polymeric backbone (which is highly unlikely, since the polymeric backbone and me-

0024-9297/89/2222-4597$01.50/0 